environmental microbiology

Environmental Microbiology (2021) **23**(8), 4489–4504 doi:10.1111/1462-2920.15642

DNA-stable isotope probing (DNA-SIP) identifies marine sponge-associated bacteria actively utilizing dissolved organic matter (DOM)

Sara Campana[1*] **Kathrin Busch**[2] **Ute Hentschel**[2] **Gerard Muyzer**[1] **and Jasper M. de Goeij**[1,3]

[1]*Department of Freshwater and Marine Ecology, Institute for Biodiversity and Ecosystem Dynamics, University of Amsterdam, P.O. Box 94240, 1090 GE Amsterdam, Netherlands.*

[2]*Department of Marine Ecology, Research Unit Marine Symbioses, GEOMAR Helmholtz Centre for Ocean Research Kiel, Düsternbrooker Weg 20, 24105 Kiel, Germany.*

[3]*CARMABI Foundation, Piscaderabaai z/n, P.O. Box 2090, Willemstad, Curaçao.*

Summary

Sponges possess exceptionally diverse associated microbial communities and play a major role in (re) cycling of dissolved organic matter (DOM) in marine ecosystems. Linking sponge-associated community structure with DOM utilization is essential to understand host–microbe interactions in the uptake, processing, and exchange of resources. We coupled, for the first time, DNA-stable isotope probing (DNA-SIP) with 16S rRNA amplicon sequencing in a sponge holobiont to identify which symbiotic bacterial taxa are metabolically active in DOM uptake. Parallel incubation experiments with the sponge *Plakortis angulospiculatus* were amended with equimolar quantities of unlabelled (^{12}C) and labelled (^{13}C) DOM. Seven bacterial amplicon sequence variants (ASVs), belonging to the phyla PAUC34f, Proteobacteria, Poribacteria, Nitrospirae, and Chloroflexi, were identified as the first active consumers of DOM. Our results support the predictions that PAUC34f, Poribacteria, and Chloroflexi are capable of organic matter degradation through heterotrophic carbon metabolism, while Nitrospirae may have a potential mixotrophic metabolism. We present a new analytical application of DNA-SIP to detect substrate incorporation into a marine holobiont with a complex associated bacterial community and provide new experimental evidence that links the identity of diverse sponge-associated bacteria to the consumption of DOM.

Received 10 February, 2021; revised 11 June, 2021; accepted 11 June, 2021. *For correspondence. E-mail s.campana@uva.nl; Tel. (+31) 0 205256408, Fax: (+31) 020 525 7832.

[Corrections added on 13 July 2021, after first online publication date: In the article title, ‘‘DNA-stable isotope probing’’ was mentioned twice and has been removed in this version.]

Introduction

Sponges are among the oldest extant metazoans and a unique model system to study early metazoan–microbe interactions because of their exceptionally diverse associated microbial communities (Thomas *et al*., 2016; Moitinho-Silva *et al*., 2017a). Sponge holobionts, consisting of the sponge host and its associated microbiota, are important aquatic ecosystem drivers because of their efficient filtering system, their interactions with surrounding organisms and within the holobiont itself in terms of nutrient cycling and providing habitat (Webster and Taylor, 2012; Webster and Thomas, 2016; de Goeij *et al*., 2017; Pita *et al*., 2018). In the oceans, primary producers, such as phytoplankton, macroalgae, and dinoflagellates in corals release the product of their photosynthetic activity in the form of dissolved organic matter (DOM), which is the main pool of organic matter in seawater and an important food source for sponges (Tanaka *et al*., 2011; de Goeij *et al*., 2013; Thornton, 2014; Hansell and Carlson, 2015; Rix *et al*., 2017; Bart *et al*., 2020). In fact, dissolved organic carbon (DOC) – a component of the DOM pool – can contribute to 60%–97% of the daily carbon intake of sponges (Yahel *et al*., 2003; de Goeij *et al*., 2008; Mueller *et al*., 2014; Hoer *et al*., 2018; McMurray *et al*., 2018). Sponges consume DOM and release particulate organic matter as detritus, which is readily available to higher trophic levels (de Goeij *et al*., 2013) or stored as biomass, which is hypothesized to be predated upon by spongivores (McMurray *et al*., 2018). This so-called sponge loop is of high ecological relevance in tropical coral reefs where sponges are estimated to cycle DOC in the same order of magnitude as the primary production

rates of the entire ecosystems (de Goeij *et al*., 2013). In the deep-sea, sponges are also very abundant, forming large sponge-dominated ecosystems called sponge grounds (Maldonado *et al*., 2017), or as part of cold-water coral reefs (Cathalot *et al*., 2015). The processing of DOM by deep-sea sponges has been experimentally confirmed (Rix *et al*., 2016; Leys *et al*., 2018; Maier *et al*., 2020; Bart *et al*., 2020; Bart *et al*., 2021), but the ecological relevance is not yet established.

Organic and inorganic nutrient uptake (from here on collectively called 'nutrients') is believed to occur through a symbiotic relationship within the sponge holobiont with reciprocal translocation of resources: the sponge microbiota can benefit by a supply of nutrients, such as ammonia, released by the host, while the host can profit from the internal nutrient supply performed by the diverse microbial metabolism (Taylor *et al*., 2007; Hentschel *et al*., 2012; Webster and Taylor, 2012; Zhang *et al*., 2019). Although the proposed symbiotic functions are extensive and mostly described for photoautotrophic nutrient cycling within the sponge holobiont (Wilkinson, 1983; Steindler *et al*., 2002; Erwin and Thacker, 2008; Weisz *et al*., 2010; Freeman and Thacker, 2011; Fiore *et al*., 2013), examples of heterotrophic interaction (e.g., the uptake and cycling of organic matter) between sponge host cells and microbial symbionts are scarce. Recent nanoscale secondary ion mass spectrometry (nanoSIMS) studies have visualized and quantified DOM assimilation by the sponge host cells and associated symbionts (Achlatis *et al*., 2019; Rix *et al*., 2020) along with the transfer of carbon and nitrogen within the holobiont (Hudspith *et al*., 2021). Both sponge holobionts with high and low abundances of microbial symbionts were found to assimilate DOM, with different relative contributions of host and symbionts. Whereas microbial symbionts extensively assimilated DOM, the filter cells (choanocytes) of the sponge host also readily take up DOM (de Goeij *et al*., 2009; Achlatis *et al*., 2019; Rix *et al*., 2020) and even translocation of the assimilated DOM from the host cells to the symbionts was found (Hudspith *et al*., 2021). However, the identity of the microbial groups actively involved in DOM uptake and processing within the sponge holobiont remains unresolved.

In recent years, environmental microbiology has taken a step further in linking metabolic activity with the phylogenetic identity of uncultivated microorganisms through the development of stable isotope-based techniques coupled with next generation sequencing. The principle of stable isotope probing (SIP) is to amend an experimental incubation with a substrate labelled with a heavy stable isotope (e.g., ^{13}C or ^{15}N) and track the labelled compounds into cellular biomass components, like DNA or RNA (Radajewski *et al*., 2000; Dumont and Murrell, 2005; Whiteley *et al*., 2007; Neufeld *et al*., 2007a). A long ultracentrifugation step (36–65 h) creates a density gradient along which the cellular components labelled by the heavy isotope can be isolated into multiple fractions and sequenced, thus linking the identity of the organisms to the uptake of specific substrates or to specific metabolic functions (Radajewski *et al*., 2000; Neufeld *et al*., 2007a). In the marine environment, SIP has been used to identify bacterioplankton taxa incorporating readily bioavailable DOM as opposed to the refractory component of DOM, which generally comprises 75%–90% of the DOM pool (Nelson and Carlson, 2012; Bryson *et al*., 2017; Liu *et al*., 2020). SIP is therefore a promising approach to track direct incorporation of DOM into the biomass of responding microbial populations and to understand DOM metabolism in the sponge microbiota. Here, we conducted for the first time a DNA-SIP experiment in the sponge *Plakortis angulospiculatus* (Porifera, Homoscleromorpha) to investigate which of the associated bacterial taxa can actively incorporate DOM. The species *P. angulospiculatus* was chosen because it is widespread across the Caribbean and contains a high abundance of associated microbes (Hudspith *et al*., 2021). Seven bacterial amplicon sequence variants (ASVs) belonging to the phyla PAUC34f, Proteobacteria, Poribacteria, Nitrospirae, and Chloroflexi were identified as active DOM processors in *P. angulospiculatus*, therefore providing new experimental evidence of their ecological roles in the sponge holobiont.

Experimental procedures

Collection and maintenance of sponges

Individuals of the sponge *Plakortis angulospiculatus* were collected by SCUBA diving from between 5 and 30 m water depth on the fringing reef close to Piscadera Bay on Curaçao (12°12' N, 68°96' W). All experimental work was conducted at the CARMABI Research Station between May and August 2018. Collection and experiments were performed under the research permit (#2012/48584) issued by the Curaçaoan Ministry of Health, Environment and Nature (GMN) to the CARMABI Foundation. After collection, sponge individuals were trimmed to sizes of 8–10 cm^3 with at least two functioning oscula (i.e., outflow opening; active pumping tested with fluorescent dye) and cleared from epibionts. The sponges were immediately transported without air exposure to the CARMABI aquarium facilities and kept in 100 l flow-through aquaria, with a flow rate of 3 l min^{-1}, supplied with seawater pumped directly from the reef at 10 m water depth. All individuals were allowed to recover from tissue damage caused by the initial trimming and to acclimatize in the aquaria up to 4 weeks prior to incubation experiments (Alexander *et al*., 2015). Only visually

healthy individuals (actively pumping, with open oscula) were used in the experiments.

SIP incubations

Two different treatments were amended: ^{12}C-unlabelled DOM and ^{13}C-labelled DOM. Per treatment, three sponge replicates and one seawater control without sponge were incubated. The added tracer-DOM was extracted from 1 g of unlabelled (^{12}C) or 1 g of labelled (^{13}C) lyophilized algal cells (>98% atom purity, ULM-2177 and CLM-2065 *Agmenellum quadruplicatum*, Cambridge Isotope Laboratories). Briefly, the algal cells were resuspended in Milli-Q water, sonicated for 15–20 min and then centrifuged for 10 min at 8000*g*. Subsequently, the supernatant was first filtered over a 0.7-μm GF/F grade filter and then over a 0.2-μm polycarbonate membrane filter to remove possible algal cell remnants from the DOM solution. This process was repeated with the pellet left after the centrifugation step, in order to extract most of the DOM. The filtered DOM was freeze dried and analysed by elemental analyser–isotope ratio mass spectrometry (EA-IRMS) to determine the C and N content and isotopic composition. The freeze-dried DOM was then solubilized in ultrapure water (18.2 MΩ-cm type I, Elga Purelab Classic UV) at CARMABI Research Station prior to the incubations. Experimental incubations were carried out in 3 l incubation chambers for 6 h. The sponges were transferred, without air exposure, to air-tight, stirred, incubation chambers (de Goeij *et al*., 2013), which were filled with 0.7-μm filtered seawater (FSW). The resuspended DOM was added at the beginning of the incubation using a sterile syringe (at a final concentration of 120 μM DOC). One FSW control (without a sponge) was also incubated per treatment under the same conditions to exclude possible feeding of the sponge on enriched seawater bacterioplankton. All incubations were conducted in the dark and dissolved oxygen concentrations were monitored continuously with an optical probe (OXY-4; PreSens, Regensburg, Germany). Incubation chambers were placed in a flow-through aquarium (water pumped up from 10 m water depth from the nearby reef) to ensure near *in situ* temperatures. At the end of each incubation, the sponges were rinsed in non-labelled 0.7-μm FSW and dipped in ultrapure water to remove salts before sampling. Each sponge was cut in half, one half was kept for ^{13}C bulk tissue (i.e. holobiont tissue) stable isotope analysis, and the other half was immediately snap-frozen and stored at −80°C until DNA extraction. The seawater from each control incubations (3 l) was collected and filtered over a Sterivex filter (GP 0.22 μm) using a peristaltic pump. The Sterivex filters were stored at −80°C until DNA extraction.

Stable isotope analysis

Sponge tissue samples for bulk stable isotope analysis were weighted before (wet weight) and after freeze-drying (dry weight). Dry tissue was milled with a mortar and pestle. For each sample, a subset of thoroughly mixed tissue powder was decalcified by acidification with a few drops of fuming HCl until effervescence ceased and freeze-dried again. Duplicate (10–30 mg) acidified and non-acidified samples were transferred to tin cups for bulk ∂^{13}C isotope analysis. The carbon content and the ^{13}C/^{12}C isotopic composition was measured simultaneously with a high-temperature combustion element analyser (Vario Isotope cube, Elementar GmbH, Langenselbold, Germany) coupled with an isotope ratio mass spectrometer (BioVision, Elementar, Stockport, UK). A two-point calibration curve was used to correct the isotopic data. The ^{13}C values were measured against caffeine (IAEA-600, $\partial^{13}C = -27.77‰$) and UL-D-glucose (IAEA-309B, $\partial^{13}C = 535.3‰$), used as low and high internal stable-isotope standards, respectively. The ^{13}C stable-isotope data were calculated as previously described (Rix *et al*., 2020; Bart *et al*., 2020; for details see Supporting Information). Isotope data from the incubations are corrected for: the background ∂^{13}C values (measured in the sponges incubated with unlabelled DOM), the sponge dry weight, the incubation time, and the enrichment of the DOM source used as substrate. Isotope-tracer-DOM assimilation rates are expressed as $\mu mol\ C_{tracer}\ mmol\ C_{sponge}^{-1}\ h^{-1}$.

DNA extractions

DNA was extracted from the sponge tissue samples using the DNeasy® Blood & Tissue Kit (Qiagen). The tissue was first homogenized in 180 μl Buffer ATL and 20 μl proteinase K using a small sterile pestle that fits in a 1.5 ml microcentrifuge tube. Afterwards, all tissue samples were incubated overnight at 56°C. After the incubation, 200 μl of Buffer AL were added to each sample, followed by 200 μl of ethanol [100% (v/v)] and mixed thoroughly by vortexing. Before adding the homogenate onto the DNeasy mini spin column, all samples were centrifuged at 6000*g* for 2 min to precipitate unlysed material. The supernatant was then transferred onto the spin column and the protocol was further followed as described by the manufacturer. DNA from the Sterivex filters was also extracted using DNeasy® Blood & Tissue Kit (Qiagen). The volumes of Buffer ATL and proteinase K were doubled as deviation from the original manufactory protocol and pipetted into the filter cartridge after which the whole filter was incubated in an oven at 55°C with a sample rocker. After the incubation, 400 μl of Buffer AL were pipetted into the filter cartridge through

the luer-lock side and the filter was incubated for another 20 min at 70°C to deactivate the proteinase K. The entire volume was extracted from the cartridge using a sterile 3 ml syringe by taking it up into the syringe and transferred to a 2 ml microcentrifuge tube. Then, 400 μl of 100% (v/v) ethanol was added and after mixing by vortexing the entire sample was loaded onto the spin column. The protocol was further followed as described by the manufacturer. The concentration and purity of the extracted DNA were checked with a NanoDrop 1000™ spectrophotometer (Thermo Fischer Scientific, MA, USA).

Density gradient centrifugation and fractionation

For DNA separation, caesium chloride (CsCl) gradients were prepared as described by Neufeld *et al*. (2007a). Briefly, around 2 μg of DNA was mixed with 4.8 ml of 7.163 M CsCl solution and the appropriate gradient buffer (GB) (0.1 M Tris, 0.1 M KCl and 1 mM EDTA) volume to obtain a final density of 1.725 g ml^{-1}. The solution was transferred to a sterile 4.9 OptiSeal polypropylene centrifuge tube (Beckham Coulter, CA, USA) and centrifuged in an Optima L-90 K ultracentrifuge (Beckham Coulter) fitted with a VTi 90 rotor (Beckham Coulter), for 40 h at 177 000*g* and 20°C, with the vacuum on, maximum acceleration and deceleration without brake. After centrifugation the gradients were recovered dropwise from the bottom of the tube by injecting ultrapure water with 0.2% (v/v) of loading dye on top of the tube using a LEGATO® 100 syringe pump (KD Scientific, MA, USA) with a speed of 0.5 ml min^{-1}. A total of 15 fractions of 330 μl each were collected per sample. The refractive index (nD-TC) of each gradient fraction was measured using an AR200 digital refractometer (Reichert, NY, USA) and converted to buoyant density based on a standard curve of nD-TC versus GB-CsCl solution. The DNA from all fractions was precipitated with 1 μl of glycogen (20 μg) and two volumes of polyethylene glycol (PEG) 6000 solution. Pelleted DNA was washed with 70% (v/v) ethanol and resuspended in nuclease-free water. The DNA concentration of each fraction was measured with Qubit® dsDNA HS Assay Kit and Qubit® 2.0 Fluorometer (Invitrogen, CA, USA). DNA was stored at −20°C until further analysis. For each experimental treatment, a DNA density profile was created (Fig. 1). Equal density ranges were selected for the sponge and the seawater control profiles, based on the observed differences in the amount of DNA between labelled and unlabelled treatments. DNA fractions were grouped in the following density ranges: super heavy (fractions 2, 3, 4), heavy (fractions 5, 6, 7), medium (fractions 8, 9, 10, 11) and light (fractions 12, 13, 14), and the fractions within each range were pooled volumetrically (5 μl of each fraction). Because fraction 1 (the heaviest fraction) and fraction 15 (the lightest fraction) contain mostly CsCl or sterile water they were excluded for further analysis.

16S amplicon sequencing and data analyses

Pooled fractions of the CsCl gradient were submitted for 16S amplicon sequencing. The V3-V4 region of the 16S rRNA gene was amplified using the primer pair 341f/806r (dual-barcoding approach; Kozich *et al*., 2013; primer sequences: 5'-CCTACGGGAGGCAGCAG-3′ and 5'-GG ACTACHVGGGTWTCTAAT-3'). The PCR conditions were as follows: initial denaturation step for 30 s at 98°C, 30 cycles of denaturation for 9 s at 98°C, annealing for 30 s at 55°C and extension for 30 s at 72°C, followed by a final extension step of 10 min at 72°C. The product quality and quantity were checked using gel electrophoresis. PCR products were normalized (SequalPrep normalization plate kit; Thermo Fisher Scientific, Waltham, USA) and pooled. Amplicon libraries were sequenced using the MiSeq v3 chemistry sequencing kit (2 × 300 bp) on an Illumina MiSeq platform (MiSeq FGx; Illumina, San Diego, USA). Raw sequences were quality filtered and trimmed based on quality scores. Amplicon sequence variants (ASVs) were computed with the DADA2 algorithm within QIIME2 (version 2018.11). To train the error model, 1 million reads were used. Chloroplasts and mitochondrial sequences were removed from further analyses. Phylogenetic ASV trees were generated with the FastTree2 plugin. A primer-specific trained Naive Bayes taxonomic classifier was used to classify representative ASVs based on the Silva 132 99% OTUs 16S database. Weighted UniFrac distances were calculated and sample separation in ordination space visualized by non-metric multidimensional scaling (nMDS) in RStudio Version 1.2. Permutational multivariate analyses of variance (PERMANOVAs) were performed with 999 permutations to determine whether bacterial communities were statistically significantly different between treatments. Furthermore, significant enrichment between treatments and density fractions was determined and ranked using the linear discriminant analysis effect size (LEfSe) algorithm, with a P value of 0.05 and LDA threshold of 2 (Segata *et al*., 2011). Microbiome Analyst software (Chong *et al*., 2020; www.microbiomeanalyst.ca) was used to perform PERMANOVAs and LEfSe analyses. Among the significantly enriched taxa ($P < 0.05$, LEfSe) in the sponge-associated bacterial community, substrate incorporation was validated based on two criteria: (i) the increasing relative abundance of a taxon in the ^{13}C treatment occurs in at least two consecutive density fractions, with highest abundance in the heaviest of the two fractions, and ii) the relative abundance of the taxon in the ^{13}C treatment is greater than its relative abundance in

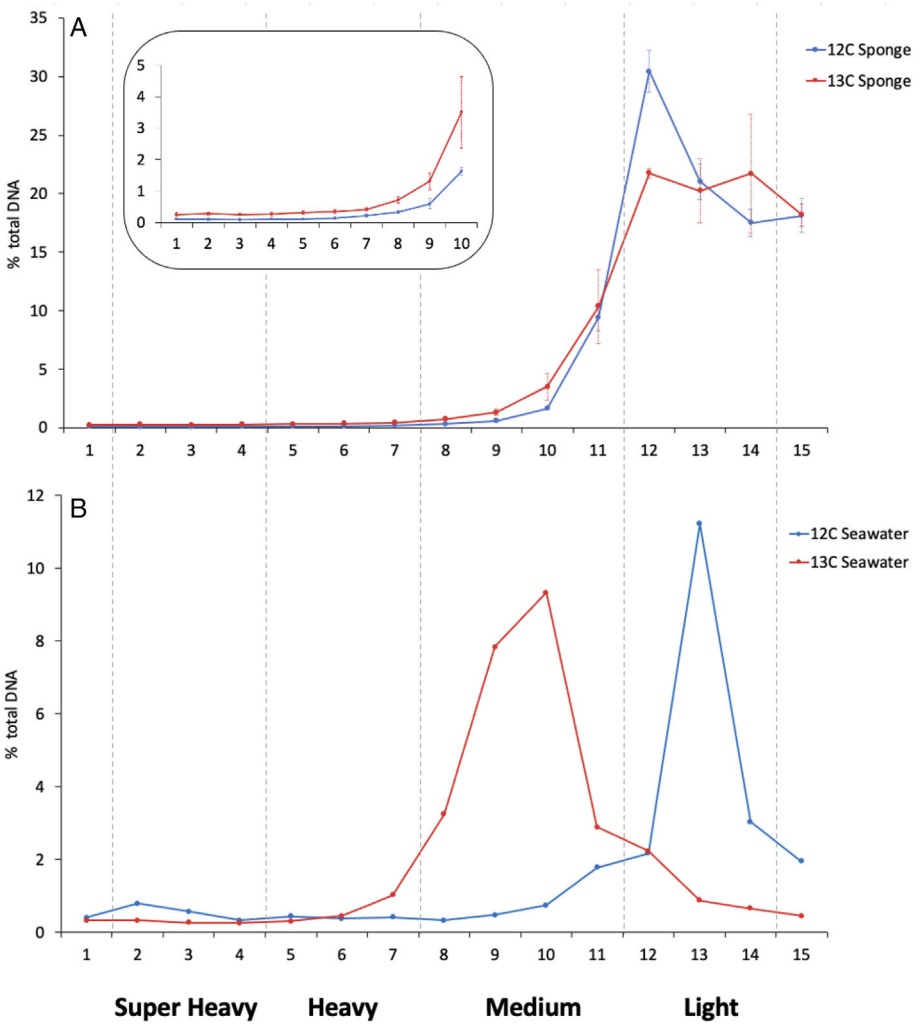

Fig 1. Distribution of the DNA in the CsCl gradients of (A) sponge DNA ($n = 3$) and (B) seawater bacterioplankton DNA ($n = 1$). The line charts show the percentage of total gradient DNA contained in each fraction of ^{12}C treatment (blue line) and ^{13}C treatment (red line) (data shown as mean % ± SD). Density ranges constituting each pooled fraction are separated by the dotted grey arrow and indicated as Super Heavy, Heavy, Medium, and Light.

the ^{12}C treatment in both density fractions. Because only one seawater sample was collected per treatment, the seawater bacterial community comparisons were only made between treatments, using the density fractions as technical replicates, and thus allowing only conclusion on taxa enrichment between treatments, but not between density fractions. Taxa detected only in one of the two treatment were removed from the enrichment analysis in order to exclude possible artefacts of the methodology itself. The sequence data have been deposited in the NCBI database under BioProject ID PRJNA698441.

Results

Stable isotope analysis

Sponge tissue was enriched with tracer-DOM in the ^{13}C treatment as compared to the ^{12}C treatment (210.97 ± 36.62 and − 18.57 ± 0.47 $\partial^{13}C$ ‰ mean ± SD, respectively), showing a mean carbon assimilation rate of 0.46 ± 0.07 µmol C_{tracer} mmol C_{sponge}^{-1} h^{-1} (mean ± SD).

Density gradient centrifugation and fractionation

The density of all fractions ranged between 1.68 and 1.77 g ml^{-1}, with a linear trend decreasing from the bottom to the top, indicating proper gradient formation (Supporting Information Fig. S1). DNA extracted from the sponge samples did not show a clear distinction in distribution when looking at the light fractions; however, in the medium and heavy fractions (see magnification panel in Fig. 1A), an increase in the DNA concentration was visible in the ^{13}C treatment as compared to the ^{12}C treatment (Fig. 1A). The distinction in DNA distribution was evident in the DNA extracted from the seawater controls, where the highest peak of DNA abundance shifted from the light fraction of the ^{12}C treatment to the medium fraction of the ^{13}C treatment (Fig. 1B).

16S amplicon sequencing

After filtering and quality control, 908 906 bacterial sequences were obtained from 32 samples, resulting in an average frequency of 28 403 sequence reads per sample. We identified 2102 bacterial amplicon single nucleotide variants (ASVs) affiliated to 23 bacterial phyla. Non-metric multidimensional scaling (nMDS) based on weighted UniFrac distances clearly separated the sponge-associated bacterial community and the seawater bacterioplankton community (Supporting Information Fig. S2). An nMDS ordination plot of the sponge-associated bacterial community alone showed a slight separation between the density fractions along the horizontal axis with heavier ones (darker shaded 'SH' and 'H') clustering to the left and lighter ones (lighter shaded 'M' and 'L') to the centre-right (Fig. 2). Overall, the three replicates of each fractions of the ^{13}C treatment were more dispersed compared with the more closely clustered replicates of the ^{12}C treatment.

Taxonomic assignment revealed that in the sponge-associated bacterial community the predominant phyla were Chloroflexi (35.9%), Proteobacteria (22.7%), Acidobacteria (14.2%), Actinobacteria (10.2%), Gemmatimonadetes (4.9%), Nitrospirae (3.8%), Spirochaetes (1.8%), Entotheonellaeota (1.7%), and PAUC34f, Poribacteria, Nitrospinae, and Dadabacteria, each accounting for 0.9% (Fig. 3A). The seawater bacterioplankton community, instead, consisted mostly of Proteobacteria accounting for 94.2% on average (Fig. 3B).

There was a significant difference in the sponge-associated bacterial community among the density fractions of the ^{13}C-labelled and ^{12}C-unlabelled DOM treatments (PERMANOVA, F-value = 1.647; R^2 = 0.42; P = 0.048). A total of 10 sponge-associated bacterial ASVs resulted significantly enriched (P < 0.05, LEfSe), of which seven in the ^{13}C treatment and three in the ^{12}C treatment (Fig. 4 and Table 1). Sponge-associated bacterial ASVs significantly enriched in the ^{13}C treatment super heavy fraction were a PAUC34f bacterium and a Proteobacteria of the genus *Endozoicomonas* (Fig. 4A and B) and in the heavy fraction a Poribacterial ASV, a *Nitrospira* genus and three ASVs belonging to the Chloroflexi SAR202 clade (Fig. 4C–G). The three sponge-associated ASVs significantly enriched in the ^{12}C super heavy fraction were an Entotheonellaeota bacterium, a PAUC26f Acidobacterium and an uncultured Chloroflexi bacterium (Fig. 4H–J). LEfSe analysis showed that four of these sponge-associated ASVs were significantly enriched at all taxonomical levels (from phylum to ASVs), namely, the Poribacteria, PAUC34f, and Nitrospirae taxa in the ^{13}C treatment and the Entotheonellaeota ASV in the ^{12}C treatment (Table 1).

A significant change was also detected between the ^{13}C and ^{12}C treatment in the seawater bacterioplankton community composition (PERMANOVA, F-value = 32.129; R^2 = 0.41; P = 0.028). Specifically, 48 ASVs were found to be significantly enriched (P < 0.05, LEfSe) in one of the two treatment, and 42 of them at all taxonomical levels

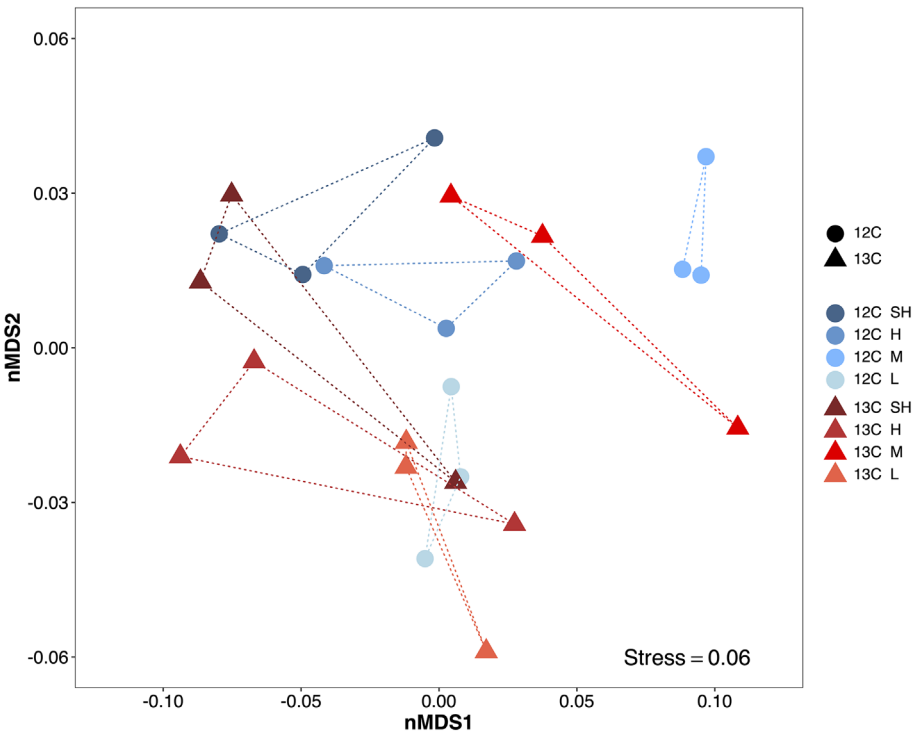

Fig 2. Sponge-associated bacterial community composition visualized by a non-metric multidimensional scaling plot on weighted UniFrac distances at the ASV level. Each marker is one bacterial community, with symbols and colours indicating the combination of treatment (^{12}C circles in shades of blue and ^{13}C triangles in shades of red) and density fractions (SH: Super Heavy, H: Heavy, M: Medium, and L: Light).

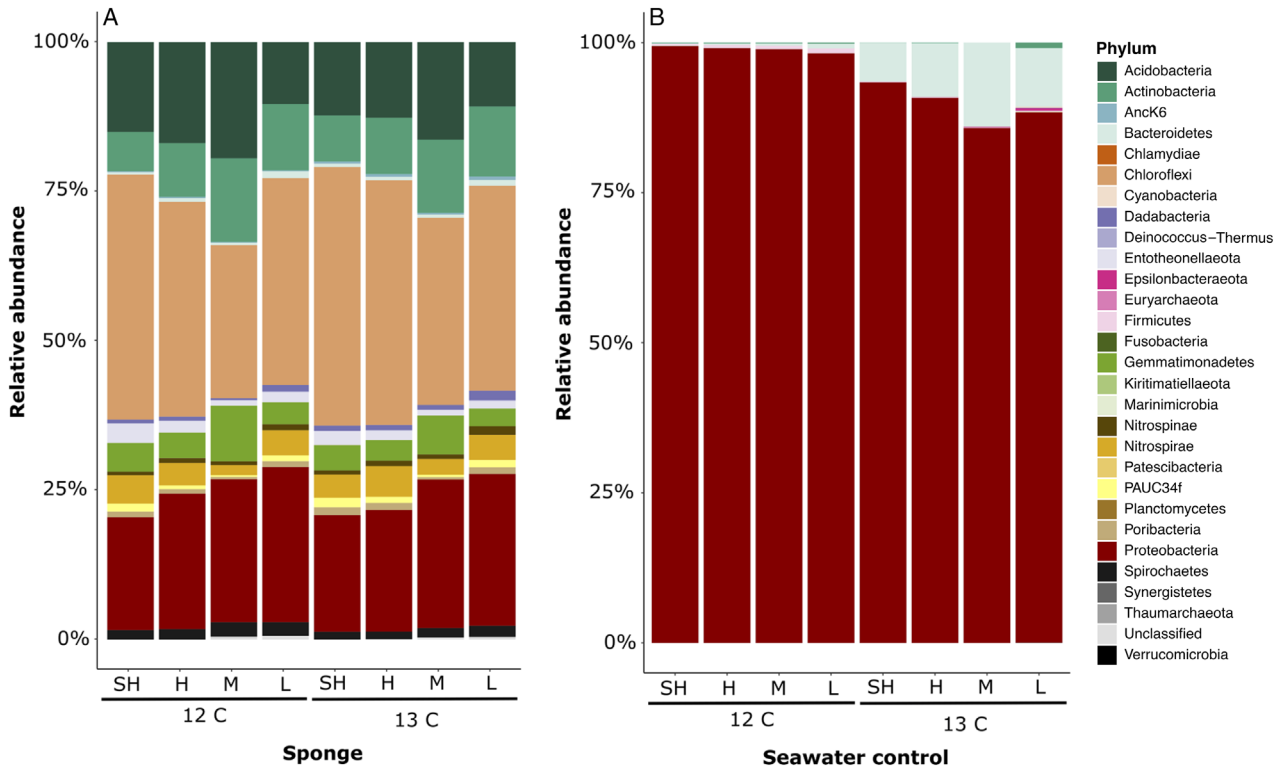

Fig 3. Relative abundance of bacterial phyla among the pooled density fraction of the ^{12}C and ^{13}C treatments in (A) the sponge-associated bacterial community and (B) the seawater control. Density fractions are indicated as SH: Super Heavy, H: Heavy, M: Medium, and L: Light.

(Table 1). The Bacteroidetes phylum was enriched in the ^{13}C treatment (9.8%) compared to ^{12}C treatment (0.4%) (Supporting Information Fig. S3a). Within this phylum, the enriched genera were *Tenacibaculum*, *Marinoscillum*, *Roseivirga*, and *Pontibacter*. The Proteobacteria phylum was overall enriched in the ^{12}C treatment (98.9%) compared to ^{13}C treatment (89.6%), however when looking at the class level a division was clear between the Alphaproteobacteria, which abundance increased in the ^{12}C treatment (27.35% vs 54.4%, ^{13}C vs ^{12}C treatment, respectively; Supporting Information Fig. S3b), and the Gammaproteobacteria, which abundance instead increased in the ^{13}C treatment (46.1% vs 34.5%; Supporting Information Fig. S3c). Ten gammaproteobacterial ASVs were enriched in the seawater ^{13}C treatment and belonged to the genera *Vibrio*, *Alteromonas*, *Thalassotalea*, *Litoricola*, *Neptuniibacter*, and *Reinekea*. One of the *Alteromonas* ASVs that resulted enriched in the seawater bacterial community was also enriched in the sponge-associated bacterial community from the order to the ASV level in the ^{13}C treatment. The other eight Gammaproteobacterial ASVs were enriched in the seawater ^{12}C treatment and belonged to the genera *Oleibacter*, *Vibrio*, *Acinetobacter*, *Pseudomonas*, *Marinobacter*, *Pseudoalteromonas*, and an uncultured *Cellvibrionaceae*. Among the Alphaproteobacteria, nine ASVs were enriched in the labelled treatment, including the genera *Thalassospira*, *Nautella*, *Pelagibaca*, *Ruegeria*, and *Thalassobius*, while 15 other alphaproteobacterial ASVs were enriched in the ^{12}C treatment, encompassing the genera *Ponticaulis*, *Shimia*, *Thalassobius*, *Tropicibacter*, a *Sphingomonadaceae* bacterium, and seven other *Rhodobacteraceae*. *Exiguobacterium* of the phylum Firmicutes was also enriched in the seawater ^{12}C treatment (Supporting Information Fig. S3d).

Discussion

DNA-SIP has been widely used in environmental microbiology, but there are only few studies that applied this technique *in vivo* to understand the role of microbes that live in symbiotic association with a host (Shao *et al*., 2014; Alonso-Pernas *et al*., 2017). To the best of our knowledge, this is the first study applying DNA-SIP to a marine holobiont. Here we linked the identity of sponge-associated bacterial taxa to their ability of incorporating DOM – a complex mixture of low- and high-molecular weight biomolecules, including proteins, lipids, and carbohydrates (Nebbioso and Piccolo, 2012) –,

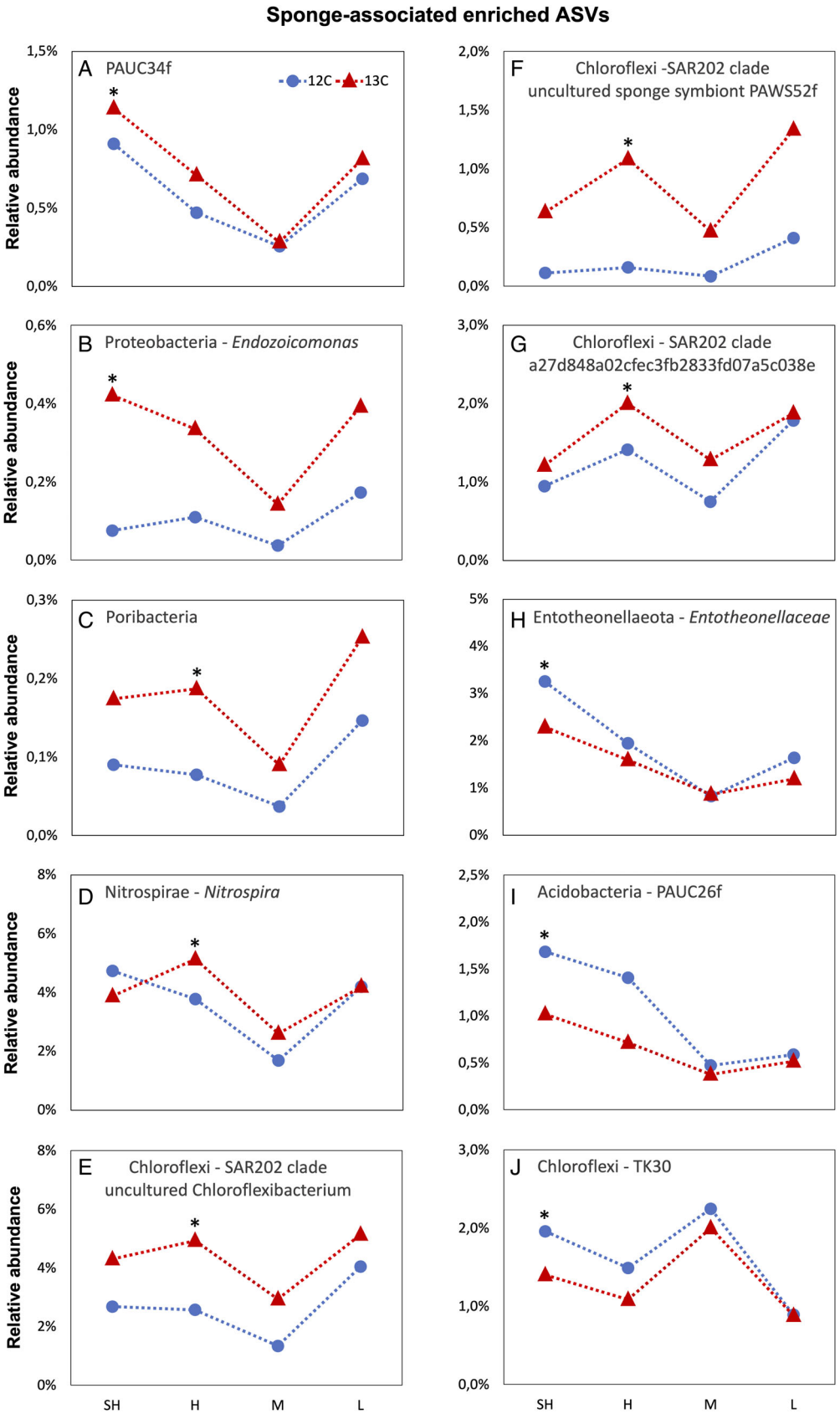

Fig 4. Legend on next page.

which is the largest source of organic matter in the oceans (Hansell and Carlson, 2015) and is largely inaccessible to other heterotrophic marine metazoans.

Stable isotope analysis, density gradient centrifugation and fractionation

The challenge of DNA-SIP experiments is employing sufficient substrate (e.g., DOM) concentration and incubation time, but staying as close as possible to the *in situ* ambient conditions (Dumont and Murrell, 2005; Neufeld *et al*., 2007b). Too short incubation times may cause insufficient above-background enrichment for the successful isolation of ^{13}C-labelled DNA (Teng-xiang *et al*., 2016), whereas too long incubation times could cause enrichment bias due to cross-feeding by secondary consumers on the metabolic by-products released by the initial consumers (Neufeld *et al*., 2007b). Experimental conditions become more unpredictable in holobionts with complex microbial communities compared to pure bacterial cultures.

The treatment conditions used in our experiment were suitable to detect isotopic enrichment in the labelled samples compared to the unlabelled ones. Furthermore, our approach resulted in isotopic enrichment and DOM incorporation rates similar to those observed in previous studies where diatom or cyanobacterial DOM was used as a labelled substrate for estimating DOM uptake and release by sponges and their associated microbes (de Goeij *et al*., 2013; Achlatis *et al*., 2019; Rix *et al*., 2020; Bart *et al*., 2020; Hudspith *et al*., 2021; Campana *et al*., 2021). The suitability of our treatment conditions was also proven by the clear shift in DNA distribution visible in the seawater bacterioplankton, indeed the highest peak of DNA abundance shifted from the light fraction in the ^{12}C treatment to the medium fraction in the ^{13}C treatment after a 6 h incubation time (Fig. 1B). This shift indicates an increase in the density of the DNA caused by the incorporation of the heavier (^{13}C) isotope by the active microbial groups, as observed previously in a DNA-SIP study on DOM uptake by Sargasso Sea bacterioplankton (Liu *et al*., 2020).

Unlike the bacterioplankton, the DNA distribution profile of the sponge bacterial symbionts did not show a clear and general shift towards heavier fractions in the ^{13}C treatment as compared to the ^{12}C treatment. Only the medium to heavier fractions became slightly heavier in the ^{13}C treatment (Fig. 1A). This could be explained by the relative low abundances of the ASVs that resulted significantly enriched in the sponge-associated bacterial community. In fact, the total difference in relative abundance between the labelled and unlabelled treatments of the significantly enriched ASVs was around 4%. Furthermore, in these samples, the extracted DNA contained both the DNA of the sponge host and its associated symbionts and we hypothesize that the host DNA was not enriched in ^{13}C as much as the DNA of the associated symbionts. For instance, in another sponge with high abundance of associated microbes, the percent contribution of host sponge cells to bulk uptake of algal tracer DOM was only 35%, with the remaining 65% assigned to the symbiont microbes (Rix *et al*., 2020). Most likely, the density shift of the bacterial DNA may have been masked by the presence of unlabelled host DNA. One option to avoid this effect could be to perform a priori cell separation of the sponge tissue before DNA extraction (Fieseler *et al*., 2006; Thomas *et al*., 2010; Freeman *et al*., 2013; Astudillo-García *et al*., 2018; Engelberts *et al*., 2020). A couple of studies have applied cell separation techniques with results reaching up to 95%–99% pure microbial fractions (Freeman *et al*., 2013; Rix *et al*., 2020) but do not report the number and composition of host and symbiont cells lost in the numerous washing steps during the process. Therefore, using separated microbial cell fractions for microbial community composition studies may not be representative of the overall microbial diversity because bacterial cells lost during the washing steps could result in a biased relative abundance of some bacterial taxa or in the complete disappearance of less abundant taxa (Fieseler *et al*., 2006). Cell separation can be nonetheless useful in (meta)genomic studies where sufficient coverage of given microbial lineages is required (Fieseler *et al*., 2006; Bayer *et al*., 2018; Mori *et al*., 2018; Schorn *et al*., 2019; Moeller *et al*., 2019). Another option to reduce host DNA contamination could be the use of methylation-based approaches, such as the NEBNext Microbiome DNA Enrichment Kit and the Molzym MolYsis Basic kit, to enrich microbial DNA after extraction (Thoendel *et al*., 2016). However, similarly to the cell separation method, there are some considerations to be made regarding this approaches. The NEBNext microbiome DNA enrichment kit has been used on one sponge species for the preparation of metagenomic libraries (Burgsdorf *et al*., 2019), but its application has not been yet optimized for the use on other sponge species. Furthermore, it is unknown whether this techniques may or

Fig 4. Relative abundance profiles of significantly enriched sponge-associated ASVs across treatments and density fractions (n = 3). A–G: Enrichment in the 13C treatment. H–J: Enrichment in the 12C treatment. Blue dots represent unlabelled fractions (12C amendments). Red triangles represent labelled fractions (13C amendments). Density fractions are indicated as SH: Super Heavy, H: Heavy, M: Medium, and L: Light. Asterisks (*) indicate in which density fraction the significant enrichment (LefSE, $P < 0.05$) was found for the sponge-associated taxa.

Table 1. Bacterial taxa that were significantly enriched in either the ^{13}C or ^{12}C treatment in the sponge-associated ($n = 3$) or in the seawater bacterial communities ($n = 1$, four technical replicates).

Taxa						Activity	LefSE ($P < 0.05$)	
Phylum	Class	Order	Family	Genus	ASV	Treatment	Sponge	Seawater
Sponge-associated								
PAUC34f	_	_	_	_	c21208a04e6186513386c2c482345edc	^{13}C SH	*	
Proteobacteria	Gammaproteobacteria	Oceanospirillales	*Endozoicomonadaceae*	*Endozoicomonas*	a2478cc476af4056defe87a849618323	^{13}C SH	**(A)	
Poribacteria	_	_	_	_	64b6cef452f5e253205a0543df547dab	^{13}C H	*	
Nitrospirae	Nitrospira	Nitrospirales	*Nitrospiraceae*	*Nitrospira*	658a5a79e887116ab355ee0a52e3dd0f	^{13}C H	*	
Chloroflexi	Dehalococcoidia	SAR202clade	Uncultured Chloroflexibacterium	Uncultured Chloroflexibacterium	60bdd0e2fee3b5ff24c4bf975df23c58	^{13}C H	*(F,G,A)	
			Uncultured sponge symbiont PAWS52f	Uncultured sponge symbiont PAWS52f	aac86c50ed061422950976fe61a5e949	^{13}C H	*(F,G,A)	
			_	_	a2478cc476af4056defe87a849618323	^{13}C H	*(A)	
Entotheonellaeota	Entotheonellia	Entotheonellales	*Entotheonellaceae*	_	c4682f3866a514d67f9fb8f721f208f5	^{12}C SH	*	
Acidobacteria	Acidobacteriia	Solibacterales	*Solibacteraceae* (Subgroup3)	PAUC26f	12f08292a37324271780e278b29d091a	^{12}C SH	*(C,O,F, G,A)	
Chloroflexi	TK30	uncultured bacterium	Uncultured bacterium	Uncultured bacterium	52ced10f6a64091cc72afd91c25f3827	^{12}C SH	*(C,O,F, G,A)	
Seawater								
Bacteroidetes	Bacteroidia	Flavobacteriales	*Flavobacteriaceae*	*Tenacibaculum*	f21f749f2b1805136d34383f8c97ece4 eff75c879b746cdcedf6afb6760e97ae 24ca9fa104b19f14339d1a7311813089	^{13}C		*
		Cytophagales	*Cyclobacteriaceae*	*Marinoscillum*	7275d37e008a936d8d5bc763e6bb4bc4	^{13}C		*
				Roseivirga	38d7233bd6197cf2336e07a3048db6cb	^{13}C		*
			Hymenobacteraceae	*Pontibacter*	e97fb331fff682a80370cee733bd1d78	^{13}C		*
Proteobacteria	Alphaproteobacteria	Caulobacterales	*Hyphomonadaceae*	*Ponticaulis*	a813833b5bf150261ffc393184d30d44 40d8840a3be2a4fe8dde5eda0476ad31	^{12}C		*
				uncultured	6de8b46c22914de5a20a9ee515922538	^{12}C		*
		Sphingomonadales	*Sphingomonadaceae*	_	561ccfc9d063356c8373a600171733ec	^{12}C		*
		Rhodobacterales	*Rhodobacteraceae*	*Shimia*	206c94637323740ba5098d13f68ca613	^{12}C		*
				Thalassobius	6dcfa855474bb1059df1cb23148cb7a7	^{12}C		*
				Tropicibacter	9f2a8d79acd772807cef2413a7eec54f	^{12}C		*
				_	01a15b2901a87b10a9c86180308bed9f 23213ccd4beac18b2bc709906fd88799 f9b669c4bc34d832d53e35560fa82bb3 07d7253127dd990ba7624c7583eae864 d465efd32b6588a04333c4ecf8cb4b12 a3db2151875b48c2902e982d93392359 ce1f4d53c75557d9f75dea813b22abf1	^{12}C		*
				Nautella	ac400ce27d3fc3110fc2470116a8ed5b	^{13}C		*
				Pelagibaca	9f90f4404e5d2136a0a3e6c7b338728d	^{13}C		*
				Ruegeria	64eb1f3c8c959ed10dcf396ed914c6f0	^{13}C		*
				Thalassobius	9bd0341d1fa5ed1bc0b72992262bc0ce 1238794ef18ee8cb8a3d859c49baff1b	^{13}C		*
				_	1ce2fdedd72ccc2531126fdddfc0a17e 5e812dd01970e02d58df8803208c4ccf 29fbbbc6e3ca28a22617dd162afcfa20	^{13}C		*
		Rhodospirillales	*Thalassospiraceae*	*Thalassospira*	0bb177fe74aef34be459e2e44c6db8aa	^{13}C		*

	Gammaproteobacteria	*Vibrionales*	*Vibrionaceae*	*Vibrio*	0d03338e4efc93449bc6fd3ff698df17	^{13}C		*(A)
		Vibrionales	*Vibrionaceae*	*Vibrio*	d236227c6c2e37e2a2e29320e7511b4a	^{12}C		*(A)
					88f99b7a436d728ba7dba26a1e76e946			
		Pseudomonadales	*Moraxellaceae*	*Acinetobacter*	ddcd85a2958ed67c1d62118ca454acec	^{12}C		*(A)
			Pseudomonadaceae	*Pseudomonas*	70bc0124178ab46e0f1ebc57a31d814e	^{12}C		*(A)
		Cellvibrionales	*Cellvibrionaceae*	uncultured	822420f29aeac1825f5e8da048d2a70b	^{12}C		*(A)
		Alteromonadales	*Marinobacteraceae*	*Marinobacter*	91ec927d4b3dd369fccbf441b0797054	^{12}C		*
			Pseudoalteromonadaceae	*Pseudoalteromonas*	4706b0f83ab177d31fead600620e5d4a	^{12}C		*
			Alteromonadaceae	*Alteromonas*	31ea5a141edff498d612057a56d03ee8	^{13}C	*(O,F,G,A)	*
					7d2144b913b1bbe6cb18a3c96aa6a8ef	^{13}C		*
				–	a599a94b6f7d82477adb108b6f536aa	^{13}C		*
					a69949ac60af0f6e6e35ca9f7f8d95d8			
			Colwelliaceae	*Thalassotalea*	46f9eaa760044af4acffa4a79c577b82	^{13}C		*
		Oceanospirillales	*Litoricolaceae*	*Litoricola*	624250452415 79aa22774efe55060a69b	^{13}C		*
					735040688932 98f99a4da53ea1bdef49			
			Nitrincolaceae	*Neptunilibacter*	3b307f4773127002 1d0f8334d4185d0e	^{13}C		*
			Saccharospirillaceae	*Reinekea*	ce54be95d7dcd5bc326bf8c67da61668	^{13}C		*
				Oleibacter	02ed0c05bcf4178b7d5bffa548811bc2	^{12}C		*
Firmicutes	Bacili	Bacillales	*FamilyXII*	*Exiguobacterium*	f2a5b9165468b028bc5ad45d02ef0a67	^{12}C		*

"*" represents significant enrichment at all listed taxonomical levels; *() represents significant enrichment only at the taxonomical level included in parenthesis where C = Class, O = Order, F = Family, G = Genus and A = ASV; Density fractions are indicated as SH: Super Heavy, H: Heavy, M: Medium, and L: Light.

may not introduce bias in relative abundance analysis, for example, due to the loss of some bacterial taxa.

Bacterial taxa actively incorporating ^{13}C-labelled DOM

To date, no clear or consistent shift in the sponge microbial community composition was found in relation to rates of DOM uptake through the sponge holobiont (Gantt *et al*., 2019). Our study demonstrates that, at least, seven sponge-associated bacterial ASVs, belonging to the phyla PAUC34f, Proteobacteria, Poribacteria, Nitrospirae, and Chloroflexi, are active incorporators of ^{13}C-labelled DOM. The relative abundance of these ASVs varied significantly among different density fractions. Higher relative abundance of a microbial taxon in the heavier fractions of the ^{13}C-labelled treatment can indicate higher metabolic activity in incorporating a certain isotope-tracer substrate, i.e. DOM in our case. Therefore, the pattern observed in our results suggest that in the sponge *P. angulospiculatus* a PAUC34f bacterium and an uncultured Proteobacteria of the genus *Endozoicomonas* could be the first DOM consumers followed by a Poribacteria, a Nitrospira and three Chloroflexi bacteria. We cannot, however, exclude that other microbial taxa present in *P. angulospiculatus* were also able to process DOM to a certain extent. In fact, a NanoSIMS study on the uptake of ^{13}C and ^{15}N-labelled DOM by the same sponge species indicated that after a 3-h pulse, about 50% of the microbial symbiont cells were enriched in ^{13}C (Hudspith *et al*., 2021). Our results rather provide direct evidence that the seven mentioned bacterial taxa had significant metabolic activity in the consumption and incorporation of the labelled carbon (^{13}C) source into their DNA within 6 h of incubation time. If other bacteria were able to take up the stable-isotope-enriched dissolved organic carbon, but not yet incorporate it into their DNA, the isotopic signal could be detected by NanoSIMS but missed with the DNA-SIP method in the observed time frame. Longer DNA-SIP incubations may allow to identify sponge-associated incorporating taxa with slower division time, but cofounding results could occur. Hudspith *et al*. (2021) found that there is translocation of DOM processed by sponge cells – predominantly the 'choanocytes' or sponge filter cells – to the microbial symbionts 48 h after a 3-h pulse with ^{13}C/^{15}N-labelled DOM. It would be challenging to distinguish direct microbial processing of DOM versus translocated host metabolites. The bacterial taxa enriched in the sponge-associated bacterial communities differed from those enriched in the seawater control; therefore, we can exclude an enrichment bias caused by sponge feeding on the seawater bacterioplankton. The only sign of potential seawater bacteria ingestion by the sponge was the enrichment of the *Alteromonas* ASV in the ^{13}C-labelled treatment of both sponge and seawater bacterial communities (Table 1). Therefore, we did not consider the *Alteromonas* ASV as an indication of endosymbiotic processing of DOM.

To further relate the uptake of certain organic compounds from the DOM pool to the enriched bacterial taxa in the ^{13}C treatment, we can assess their reconstructed metabolic pathways as heterotrophic carbon consumers. The metabolic reconstruction of two metagenome-assembled genomes (MAGs) of PAUC34f, also known as sponge-associated unclassified lineage (SAUL), suggests that the members of this phylum possess genes involved in the tricarboxylic acid cycle (TCA), glycolysis, pentose phosphate pathway, Wood–Ljungdahl pathway, and oxidative phosphorylation (Astudillo-García *et al*., 2018). Moreover, genes encoding glycoside hydrolases (GH), glycoside transferases (GT), polysaccharide lyases (PL) and carbohydrate esterases (CE) were also present, suggesting the ability of PAUC34f to degrade glycolipids, glycopeptides and glycoproteins, compounds typically found within the sponge mesohyl and as dissolved organic matter in seawater (Blunt *et al*., 2011; Astudillo-García *et al*., 2018). *Endozoicomonas* bacteria of the phylum Proteobacteria are globally distributed endosymbionts and their genomes have been found enriched in genes for carbon sugar transport, indicating a potential role in the cycling of carbohydrates to their host (Neave *et al*., 2017). The Poribacteria phylum, originally discovered and described in marine sponges (Fieseler *et al*., 2004), has a well-described genomic repertoire (Siegl *et al*., 2011; Giles *et al*., 2013; Kamke *et al*., 2014; Slaby *et al*., 2017; Podell *et al*., 2018). The predicted functions of the central carbohydrate metabolism of Poribacteria include complete pathways for glycolysis, oxidative phosphorylation, the TCA cycle, branches of the pentose phosphate pathway, and carbon fixation via the Wood–Ljungdahl pathway (Podell *et al*., 2018). Furthermore, polysaccharides and other complex carbohydrate degradation pathways can be carried out by polysaccharide lyases, and glycoside hydrolases (GH); the genes encoding these enzymes are abundantly present in the genomes of Poribacteria (Kamke *et al*., 2013; Podell *et al*., 2018; Robbins *et al*., 2021). In analogy with the PAUC34f and the Poribacteria, the metabolism of the Chloroflexi SAR202 clade includes glycolysis, TCA cycle, pentose phosphate pathway and the respiratory chain as energy-producing pathways, additionally, autotrophic carbon fixation via the reductive citrate acid cycle and the Wood–Ljungdahl pathway were also identified (Bayer *et al*., 2018). A relevant metabolic specialization in SAR202 is the potential to degrade recalcitrant DOM, due to a large repertoire of oxidative enzymes that may help in the oxidation of recalcitrant alicyclic ring structures to more labile carboxylic acid (Landry *et al*., 2017; Bayer

et al., 2018). The reconstructed genome of a member of the sponge-associated genus *Nitrospira* proposes an autotrophic carbon metabolism via the reductive TCA (rTCA) cycle (Moitinho-Silva *et al*., 2017b). Nonetheless, there is some evidence of a possible mixotrophic lifestyle, indeed some *Nitrospira* from marine ecosystems or activated sludge can use simple organic substrates, such as pyruvate, acetate, formate and glycerol for carbon assimilation, but pure heterotrophic growth has not been observed yet (Lucker *et al*., 2010; Koch *et al*., 2015; Pachiadaki *et al*., 2017).

The Bacteroidetes phylum was the most active consumer of DOM in the (0.7-μm filtered) seawater bacterioplankton. The Proteobacteria phylum was overall enriched in the ^{12}C treatment, but when looking at lower taxonomic level we can see differential activities between members of the Alphaproteobacteria and Gammaproteobacteria, with the latter being the most active in the ^{13}C treatment. It is well recognized that Bacteroidetes (especially Cytophagales and Flavobacteriales) and Gammaproteobacteria are able to mineralize organic aggregates, such as cellulose and chitin, which are compounds that are often found in the high-molecular mass (HMW) fraction of DOM (Kirchman, 2002; Edwards *et al*., 2010). Our bacterioplankton observation, however, serves here mainly as control to distinguish sponge bacterial symbionts from seawater bacteria and indicate possible bacterioplankton feeding as opposed to endosymbiont processing of DOM. The limited replication and the filtration over a 0.7-μm filter (that likely changed the ambient bacterioplankton community composition) of our seawater control prevents solid ecological conclusions from the bacterioplankton treatment. Previous studies have assessed the uptake of different types of DOM by bacterioplankton community of the Sargasso Sea through DNA-SIP, showing that a wide variety of taxa (among which several groups of the Proteobacteria, Flavobacteria, Actinobacteria and Verrucomicrobia) are capable of incorporating DOM, and that the quality and type of DOM influences the response of these taxa in incorporating such DOM (Nelson and Carlson, 2012; Liu *et al*., 2020). Likewise, DNA-SIP can become a powerful tool to understand which sponge-associated microbial groups mediate the uptake of DOM released by different primary producers present on coral reefs, such as macroalgae, and corals.

Most of the DOM incorporating taxa identified in *P. angulospiculatus* are characteristic taxa of high microbial abundance (HMA) sponges. In HMA sponges, the bacteria can constitute up to 40% of their biomass and have a distinctive community composition, while sponges with low-microbial abundance of associated microbes, i.e., low microbial abundance (LMA) sponges, generally possess a microbial community similar to that of the seawater in both composition and abundance (Taylor *et al*., 2007; Moitinho-Silva *et al*., 2017b; Gantt *et al*., 2019). DOM-uptake strategies within the sponge holobiont have been shown to vary between LMA and HMA sponges: while the LMA sponge *Dysidea avara* relied for more than 95% on DOM uptake by host choanocyte cells, in the HMA sponge *Aplysina aerophoba* the microbial symbionts accounted for the majority (65%) of DOM uptake (Rix *et al*., 2020). Since the microbial taxa enriched in *P. angulospiculatus* are indicator taxa of HMA sponges, our results suggests that in HMA sponges DOM incorporation may depend on specific microbial taxa rather than on host cell uptake. However, to validate the hypothesis that sponges with different quantities of associated microbes have evolved different strategies to exploit DOM in the ocean (Rix *et al*., 2020), a similar DNA-SIP study in an LMA sponge would be necessary.

Conclusions

This manuscript, to best of our knowledge, represents the first application of a DNA-SIP experiment in combination with 16S amplicon sequencing in a marine holobiont. We identified sponge-associated bacterial taxa that are metabolically active in the uptake and processing of DOM. Seven ASVs, belonging to the phyla PAUC34f, Proteobacteria, Poribacteria, Nitrospirae and Chloroflexi were significant incorporators of DOM in *P. angulospiculatus*. PAUC34f, Poribacteria, and Chloroflexi have similar metabolic capabilities and could be directly involved in the degradation of labile and recalcitrant organic matter through heterotrophic carbon metabolism, while Nitrospirae may have an indirect role through carbon fixation of respired organic carbon or a potential mixotrophic metabolism. The DNA-SIP technology identified the first DOM-processing taxa within the holobiont and could be used in the future to trace the uptake of different types of DOM sources or other non-DOM substances in sponge–microbe interactions.

Author contributions

S.C. and J.M.G. designed the experiments. S.C. performed the experiments, analysed the samples and wrote the manuscript. S.C. and K.B. analysed the data. All authors reviewed and contributed to the manuscript writing.

Acknowledgements

The authors want to thank Meggie Hudspith, Celine Demey, Niklas Kornder, Benjamin Mueller, Mark Vermeij and the staff of CARMABI for fieldwork and logistical support, Susanne Wilken for help with the DNA-SIP protocol development, Jorien Schoorl for IRMS sample analysis at the University of Amsterdam and the Competence Centre for Genomic Analysis (CCGA) at Kiel University for 16S amplicon sequencing. This project has received funding from

the European Research Council (ERC) under the European Union's Horizon 2020 research and innovation programme (grant agreement #715513; personal grant to J.M. de Goeij).

References

Achlatis, M., Pernice, M., Green, K., de Goeij, J.M., Guagliardo, P., Kilburn, M.R., *et al*. (2019) Single-cell visualization indicates direct role of sponge host in uptake of dissolved organic matter. *Proc Royal Soc B* **286**: 2019–2153.

Alexander, B.E., Achlatis, M., Osinga, R., van der Geest, H. G., Cleutjens, J. P. M., Schutte, B., & de Goeij, J.M. (2015). Cell kinetics during regeneration in the sponge Halisarca caerulea: how local is the response to tissue damage?. *PeerJ*, **3**: e820.

Alonso-Pernas, P., Bartram, S., Arias-Cordero, E., Novoselov, A.L., Halty-deLeon, L., Shao, Y., and Boland, W. (2017) In vivo isotopic labeling of symbiotic bacteria involved in cellulose degradation and nitrogen recycling within the gut of the forest cockchafer (*Melolontha hippocastani*). *Front Microbiol* **8**: 1970.

Astudillo-García, C., Slaby, B.M., Waite, D.W., Bayer, K., Hentschel, U., and Taylor, M.W. (2018) Phylogeny and genomics of SAUL, an enigmatic bacterial lineage frequently associated with marine sponges. *Environ Microbiol* **20**: 561–576.

Bart, M.C., de Kluijver, A., Hoetjes, S., Absalah, S., Mueller, B., Kenchington, E., *et al*. (2020) Differential processing of dissolved and particulate organic matter by deep-sea sponges and their microbial symbionts. *Sci Rep* **10**: 17515.

Bart, M.C., Mueller, B., Rombouts, T., van de Ven, C., Tompkins, G.J., Osinga, R., *et al*. (2021) Dissolved organic carbon (DOC) is essential to balance the metabolic demands of four dominant North-Atlantic deep-sea sponges. *Limnol Oceanogr* **66**: 925–938.

Bayer, K., Jahn, M.T., Slaby, B.M., Moitinho-Silva, L., and Hentschel, U. (2018) Marine sponges as *Chloroflexi* hot spots: genomic insights and high-resolution visualization of an abundant and diverse symbiotic clade. *mSystems* **3**: e00150–e00118.

Blunt, J.W., Copp, B.R., Munro, M.H.G., Northcote, P.T., and Prinsep, M.R. (2011) Marine natural products. *Nat Prod Rep* **28**: 196–268.

Burgsdorf, I., Handley, K.M., Bar-Shalom, R., Erwin, P.M., and Steindler, L. (2019) Life at home and on the roam: genomic adaptions reflect the dual lifestyle of an intracellular, facultative symbiont. *mSystems* **4**: e00057–e00019.

Bryson, S., Li, Z., Chavez, F., Weber, P.K., Pett-Ridge, J., Hettich, R.L., *et al*. (2017) Phylogenetically conserved resource partitioning in the coastal microbial loop. *ISME J* **11**: 2781–2792.

Campana, S., Husdpith, M., Lankes, D., de Kluijver, A., Demey, C., Schoorl, J., Absalah, S., van der Meer, M. T. J., Mueller, B., & de Goeij, J. M. (2021). Processing of naturally sourced macroalgal- and coral-dissolved organic matter (DOM) by high and low microbial abundance encrusting sponges. *Front Mar Sci*, **8**: 452.

Cathalot, C., van Oevelen, D., Cox, T.J.S., Kutti, T., Lavaleye, M., Duineveld, G., and Meysman, F.J.R. (2015) Cold-water coral reefs and adjacent sponge grounds: hotspots of benthic respiration and organic carbon cycling in the deep sea. *Front Mar Sci* **2**: 37.

Chong, J., Liu, P., Zhou, G., and Xia, J. (2020) Using microbiome analyst for comprehensive stastistical, functional, and meta-analysis of microbiome data. *Nat Protocols* **15**: 799–821.

de Goeij, J.M., van den Berg, H., van Oostveen, M.M., Epping, E.H.G., and van Duyl, F.C. (2008) Major bulk dissolved organic carbon (DOC) removal by encrusting coral reef cavity sponges. *Mar Ecol Prog Ser* **357**: 139–151.

de Goeij, J.M., De Kluijver, A., Van Duyl, F.C., Vacelet, J., Wijffels, R.H., De Goeij, A.F.P.M., *et al*. (2009) Cell kinetics of the marine sponge *Halisarca caerulea* reveal rapid cell turnover and shedding. *J Exp Biol* **212**: 3892–3900.

de Goeij, J.M., Lesser, M.P., and Pawlik, J.R. (2017) Nutrient fluxes and ecological functions of coral reef sponges in a changing ocean. In *Climate Change*, Ocean Acidification and Sponges: Impacts across Multiple Levels of Organization, Carballo, J.L., and Bell, J.J. (eds). Cham: Springer International Publishing, pp. 373–410.

de Goeij, J.M., van Oevelen, D., Vermeij, M.J.A., Osinga, R., Middelburg, J.J., de Goeij, A.F.P.M., and Admiraal, W. (2013) Surviving in a marine desert: the sponge loop retains resources within coral reefs. *Science* **342**: 108–110.

Dumont, M.G., and Murrell, J.C. (2005) Stable isotope probing - linking microbial identity to function. *Nat Rev Microbiol* **3**: 499–504.

Edwards, J.L., Smith, D.L., Connolly, J., McDonald, J.E., Cox, M.J., Joint, I., *et al*. (2010) Identification of carbohydrate metabolism genes in the metagenome of a marine biofilm community shown to be dominated by *Gammaproteobacteria* and *Bacteroidetes*. *Genes* **1**: 371–384.

Engelberts, J.P., Robbins, S.J., de Goeij, J.M., Aranda, M., Bell, S.C., and Webster, N.S. (2020) Characterization of a sponge microbiome using an integrative genome-centric approach. *ISME J* **14**: 1100–1110.

Erwin, P.M., and Thacker, R.W. (2008) Phototrophic nutrition and symbiont diversity of two Caribbean sponge–cyanobacteria symbioses. *Mar Ecol Prog Ser* **362**: 139–147.

Fieseler, L., Horn, M., Wagner, M., and Hentschel, U. (2004) Discovery of the novel candidate phylum '*Poribacteria*' in marine sponges. *Appl Environ Microbiol* **70**: 3724–3732.

Fieseler, L., Quaiser, A., Schleper, C., and Hentschel, U. (2006) Analysis of the first genome fragment from the marine sponge-associated, novel candidate phylum *Poribacteria* by environmental genomics. *Environ Microbiol* **8**: 612–624.

Fiore, C.L., Jarett, J.K., and Lesser, M.P. (2013) Symbiotic prokaryotic communities from different populations of the giant barrel sponge, *Xestospongia muta*. *MicrobiologyOpen* **2**: 938–952.

Freeman, C.J., and Thacker, R.W. (2011) Complex interactions between marine sponges and their symbiotic microbial communities. *Limnol Oceanogr* **56**: 1577–1586.

Freeman, C.J., Thacker, R.W., Baker, D.M., and Fogel, M.L. (2013) Quality or quantity: is nutrient transfer driven more by symbiont identity and productivity than by symbiont abundance? *ISME J* **7**: 1116–1125.

Gantt, S.E., McMurray, S.E., Stubler, A.D., Finelli, C.M., Pawlik, J.R., and Erwin, P.M. (2019) Testing the relationship between microbiome composition and flux of carbon and nutrients in Caribbean coral reef sponges. *Microbiome* **7**: 124.

Giles, E.C., Kamke, J., Moitinho-Silva, L., Taylor, M.W., Hentschel, U., Ravasi, T., and Schmitt, S. (2013) Bacterial community profiles in low microbial abundance sponges. *FEMS Microbiol Ecol* **83**: 232–241.

Hansell, D.A., and Carlson, C.A. (2015) *Biogeochemistry of Marine Dissolved Organic Matter*, 2nd ed. Amsterdam: Academic Press, p. 693.

Hentschel, U., Piel, J., Degnan, S.M., and Taylor, M.W. (2012) Genomic insights into the marine sponge microbiome. *Nat Rev* **10**: 641–654.

Hoer, D.R., Gibson, P.J., Tommerdahl, J.P., Lindquist, N.L., and Martens, C.S. (2018) Consumption of dissolved organic carbon by Caribbean reef sponges. *Limnol Oceanogr* **63**: 337–351.

Hudspith, M., Rix, L., Achlatis, M., Bougoure, J., Guagliardo, P., Clode, P.L., *et al*. (2021) Subcellular view of host–microbiome nutrient exchange in sponges: insights into the ecological success of an early metazoan–microbe symbiosis. *Microbiome* **9**: 44.

Kamke, J., Rinke, C., Schwientek, P., Mavromatis, K., Ivanova, N., Sczyrba, A., *et al*. (2014) The candidate phylum Poribacteria by single-cell genomics: new insights into phylogeny, cell-compartmentation, eukaryote-like repeat proteins, and other genomic features. *PLoS One* **9**: e87353.

Kamke, J., Sczyrba, A., Ivanova, N., Schwientek, P., Rinke, C., Mavromatis, K., *et al*. (2013) Single-cell genomics reveals complex carbohydrate degradation patterns in poribacterial symbionts of marine sponges. *ISME J* **7**: 2287–2300.

Kirchman, D.L. (2002) The ecology of *Cytophaga–Flavobacteria* in aquatic environments. *FEMS Microbiol Ecol* **39**: 91–100.

Koch, H., Lücker, S., Albertsen, M., Kitzinger, K., Herbold, C., Spieck, E., *et al*. (2015) Expanded metabolic versatility of ubiquitous nitrite-oxidizing bacteria from the genus *Nitrospira*. *Proc Natl Acad Sci USA* **112**: 11371–11376.

Kozich, J.J., Westcott, S.L., Baxter, N.T., Highlander, S.K., and Schloss, P.D. (2013) Development of a dual-index sequencing strategy and curation pipeline for analyzing amplicon sequence data on the MiSeq Illumina sequencing platform. *Appl Environ Microbiol* **79**: 5112–5120.

Landry, Z., Swan, B.K., Herndl, G.J., Stepanauskas, R., and Giovannoni, S.J. (2017) SAR202 genomes from the dark ocean predict pathways for the oxidation of recalcitrant dissolved organic matter. *mBio* **8**: e00413–e00417.

Leys, S.P., Kahn, A.S., Fang, J.K.H., Kutti, T., and Bannister, R.J. (2018) Phagocytosis of microbial symbionts balances the carbon and nitrogen budget for the deep-water boreal sponge *Geodia barretti*. *Limnol Oceanogr* **63**: 187–202.

Liu, S., Baetge, N., Comstock, J., Opalk, K., Parsons, R., Halewood, E., and English, C.J. (2020) Stable isotope probing identifies bacterioplankton lineages capable of utilizing dissolved organic matter across a range of bioavailability. *Front Microbiol* **11**: 580397.

Lucker, S., Wagner, M., Maixner, F., Pelletier, E., Koch, H., Vacherie, B., *et al*. (2010) A *Nitrospira* metagenome illuminates the physiology and evolution of globally important nitrite-oxidizing bacteria. *Proc Natl Acad Sci U S A* **107**: 13479–13484.

Maier, S.R., Kutti, T., Bannister, R.J., Fang, J.K., van Breugel, P., van Rijswijk, P., and van Oevelen, D. (2020) Recycling pathways in cold-water coral reefs: use of dissolved organic matter and bacteria by key suspension feeding taxa. *Sci Rep* **10**: 9942.

Maldonado, M., Aguilar, R., Bannister, R., Bell, J., Conway, J., Dayton, P., *et al*. (2017) Sponge grounds as key marine habitats: a synthetic review of types, structure, functional roles, and conservation concerns. In *Marine Animal Forests: The Ecology of Benthic Biodiversity*, Rossi, S., Bramanti, L., Gori, A., and Orejas, C. (eds). Cham: Springer, pp. 145–183.

McMurray, S.E., Stubler, A.D., Erwin, P.M., Finelli, C.M., and Pawlik, J.R. (2018) A test of the sponge-loop hypothesis for emergent Caribbean reef sponges. *Mar Ecol Prog Ser* **588**: 1–14.

Moeller, F.U., Webster, N.S., Herbold, C.W., Behnam, F., Domman, D., Albertsen, M., *et al*. (2019) Characterization of a thaumarchaeal symbiont that drives incomplete nitrification in the tropical sponge *Ianthella basta*. *Environ Microbiol* **21**: 3831–3854.

Moitinho-Silva, L., Nielsen, S., Amir, A., Gonzalez, A., Ackermann, G.L., Cerrano, C., *et al*. (2017a) The sponge microbiome project. *GigaScience* **6**: 1–7.

Moitinho-Silva, L., Steinert, G., Nielsen, S., Hardoim, C.C.P., Wu, Y., McCormack, G.P., *et al*. (2017b) Predicting the HMA-LMA status in marine sponges by machine learning. *Front Microbiol* **8**: 752.

Mori, T., Cahn, J.K.B., Wilson, M.C., Meoded, R.A., Wiebach, V., Martinez, A.F.C., *et al*. (2018) Single-bacterial genomics validates rich and varied specialized metabolism of uncultivated *Entotheonella* sponge symbionts. *Proc Natl Acad Sci USA* **115**: 1718–1723.

Mueller, B., de Goeij, J.M., Vermeij, M.J.A., Mulders, Y., van der Ent, E., Ribes, M., and van Duyl, F.C. (2014) Natural diet of coral-excavating sponges consists mainly of dissolved organic carbon (DOC). *PLoS One* **9**: e90152.

Neave, M.J., Michell, C.T., Apprill, A., and Voolstra, C.R. (2017) *Endozoicomonas* genomes reveal functional adaptation and plasticity in bacterial strains symbiotically associated with diverse marine hosts. *Sci Rep* **7**: 40579.

Nebbioso, A., and Piccolo, A. (2012) Molecular characterization of dissolved organic matter (DOM): a critical review. *Anal Bioanal Chem* **405**: 109–124.

Nelson, C.E., and Carlson, C.A. (2012) Tracking differential incorporation of dissolved organic carbon types among diverse lineages of Sargasso Sea bacterioplankton. *Environ Microbiol* **14**: 1500–1516.

Neufeld, J.D., Vohra, J., Dumont, M.G., Lueders, T., Manefield, M., Friedrich, M.W., and Murrell, J.C. (2007a) DNA stable-isotope probing. *Nat Prot* **2**: 860–866.

Neufeld, J.D., Wagner, M., and Murrell, J.C. (2007b) Who eats what, where and when? Isotope-labelling experiments are coming of age. *ISME J* **1**: 103–110.

Pachiadaki, M.G., Sintes, E., Bergauer, K., Brown, J.M., Record, N.R., Swan, B.K., *et al*. (2017) Major role of nitrite-oxidizing bacteria in dark ocean carbon fixation. *Science* **358**: 1046–1051.

Pita, L., Rix, L., Slaby, B.M., Franke, A., and Hentschel, U. (2018) The sponge holobiont in a changing ocean: from microbes to ecosystems. *Microbiome* **6**: 46.

Podell, S., Blanton, J.M., Neu, A., Agarwal, V., Biggs, J.S., Moore, B.S., and Allen, E.E. (2018) Pangenomic comparison of globally distributed Poribacteria associated with sponge hosts and marine particles. *ISME J* **13**: 468–481.

Radajewski, S., Ineson, P., Parekh, N.R., and Murrell, J.C. (2000) Stable-isotope probing as a tool in microbial ecology. *Nature* **403**: 646–649.

Rix, L., de Goeij, J.M., van Oevelen, D., Struck, U., Al-Horani, F.A., Wild, C., and Naumann, M.S. (2017) Differential recycling of coral and algal dissolved organic matter via the sponge loop. *Funct Ecol* **31**: 778–789.

Rix, L., Ribes, M., Coma, R., Jahn, M.T., de Goeij, J.M., van Oevelen, D., *et al*. (2020) Heterotrophy in the earliest gut: a single-cell view of heterotrophic carbon and nitrogen assimilation in sponge-microbe symbioses. *ISME J* **14**: 2554–2567.

Rix, L., de Goeij, J.M., Mueller, C.E., Struck, U., Middelburg, J.J., van Duyl, F.C., *et al*. (2016) Coral mucus fuels the sponge loop in warm- and cold-water coral reef ecosystems. *Sci Rep* **6**: 18715.

Robbins, S.J., Song, W., Engelberts, J.P., Glasl, B., Slaby, B. M., Boyd, J., *et al*. (2021) A genomic view of the microbiome of coral reef demosponges. *ISME J* **15**: 1641–1654.

Schorn, M.A., Jordan, P.A., Podell, S., Blanton, J.M., Agarwal, V., Biggs, J.S., *et al*. (2019) Comparative genomics of Cyanobacterial Symbionts reveals distinct specialized metabolism in tropical *Dysideidae* sponges. *mBio* **10**: e00821–e00819.

Segata, N., Izard, J., Waldron, L., Gevers, D., Miropolsky, L., Garrett, W.S., and Huttenhower, C. (2011) Metagenomic biomarker discovery and explanation. *Genome Biol* **12**: R60.

Shao, Y., Arias-Cordero, E., Guo, H., Bartram, S., and Boland, W. (2014) In vivo pyro-SIP assessing active gut microbiota of the cotton leafworm, *Spodoptera littoralis*. *PLoS One* **9**: e85948.

Siegl, A., Kamke, J., Hochmuth, T., Piel, J., Richter, M., Liang, C., *et al*. (2011) Single-cell genomics reveals the lifestyle of Poribacteria, a candidate phylum symbiotically associated with marine sponges. *ISME J* **5**: 61–70.

Slaby, B.M., Hackl, T., Horn, H., Bayer, K., and Hentschel, U. (2017) Metagenomic binning of a marine sponge microbiome reveals unity in defense but metabolic specialization. *ISME J* **11**: 2465–2478.

Steindler, L., Beer, S., and Ilan, M. (2002) Photosymbiosis in intertidal and subtidal tropical sponges. *Symbiosis* **33**: 263–273.

Tanaka, Y., Miyajima, T., Watanabe, A., Nadaoka, K., Yamamoto, T., and Ogawa, H. (2011) Distribution of dissolved organic carbon and nitrogen in a coral reef. *Coral Reefs* **30**: 533–541.

Taylor, M.W., Radax, R., Steger, D., and Wagner, M. (2007) Sponge-associated microorganisms: evolution, ecology, and biotechnological potential. *Microbiol Mol Biol Rev* **71**: 295–347.

Teng-xiang, L., Guang-hua, W., Zhen-hua, Y., Xiao-bing, L., and Jian, J. (2016) Critical level of ^{13}C enrichment for the successful isolation of ^{13}C labeled DNA. *Agri Res Tech: Open Access J* **1**: 555558.

Thoendel, M., Jeraldo, P.R., Greenwood-Quaintance, K., Yao, J.Z., Chia, N., Hanssen, A.D., *et al*. (2016) Comparison of microbial DNA enrichment tools for metagenomic whole genome sequencing. *J Microbiol Methods* **127**: 141–145.

Thomas, T., Rusch, D., DeMaere, M.Z., Yung, P.Y., Lewis, M., Halpern, A., *et al*. (2010) Functional genomic signatures of sponge bacteria reveal unique and shared features of symbiosis. *ISME J* **4**: 1557–1567.

Thomas, T., Moitinho-Silva, L., Lurgi, M., Björk, J.R., Easson, C., Astudillo-García, C., *et al*. (2016) Diversity, structure and convergent evolution of the global sponge microbiome. *Nat Commun* **7**: 11870.

Thornton, D.C.O. (2014) Dissolved organic matter (DOM) release by phytoplankton in the contemporary and future ocean. *Eur J Phycol* **49**: 20–46.

Webster, N.S., and Taylor, M.W. (2012) Marine sponges and their microbial symbionts: love and other relationships. *Environ Microbiol* **14**: 335–346.

Webster, N.S., and Thomas, T. (2016) The sponge Hologenome. *mBio* **7**: e00135–e00116.

Weisz, J.B., Massaro, A.J., Ramsby, B.D., and Hill, M.S. (2010) Zooxanthellar symbionts shape host sponge trophic status through translocation of carbon. *Biol Bull* **219**: 189–197.

Whiteley, A.S., Thomson, B., Lueders, T., and Manefield, M. (2007) RNA stable-isotope probing. *Nat Prot* **2**: 838–844.

Wilkinson, C.R. (1983) Net primary productivity in coral reef sponges. *Science* **219**: 410–412.

Yahel, G., Sharp, J.H., Marie, D., Häse, C., and Genin, A. (2003) In situ feeding and element removal in the symbiont-bearing sponge *Theonella swinhoei*: bulk DOC is the major source for carbon. *Limnol Oceanogr* **48**: 141–149.

Zhang, F., Jonas, L., Lin, H., and Hill, R.T. (2019) Microbially mediated nutrient cycles in marine sponges. *FEMS Microbiol Ecol* **95**: fiz155.

Supporting Information

Additional Supporting Information may be found in the online version of this article at the publisher's web-site:

Appendix S1: supporting information